Applied Acoustics 70 (2009) 1371–1377

Contents lists available at ScienceDirect

Applied Acoustics

journal homepage: www.elsevier.com/locate/apacoust

Influence of the bridge on the vibrations of the top plate of a classical guitar

Jesús Alejandro Torres [a,*], Ricardo R. Boullosa [b]

[a] Doctorando, Ingeniería Eléctrica (Instrumentación Acústica), Facultad de Ingeniería, UNAM, Mexico
[b] Lab. de Acústica, Centro de Ciencias Aplicadas y Desarrollo Tecnológico, UNAM, Apartado Postal 70-186, Circuito Exterior s/n, Ciudad Universitaria CP 04510 D.F., Mexico

ARTICLE INFO

Article history:
Received 3 March 2009
Received in revised form 4 July 2009
Accepted 14 July 2009
Available online 6 August 2009

Keywords:
Guitar
Visualization
Bridge
Mode shapes
Operational deflection shapes

ABSTRACT

In this work the effect of two different bridge configurations on the vibrations of the top plate of a classical guitar is presented. Experimental harmonic analysis and visualization techniques, in addition to detailed damped simulations using the finite element method, were used to obtain mobility functions and operating deflection shapes of a top plate. The mobility functions were obtained in the following sequence. First the mobility functions were obtained on the top plate without a bridge attached. Then a bridge was glued to the top plate and new measurements were made. Finally the already attached bridge was cross-cut in situ without detaching it from the top plate, and the measurements were repeated. Those specific designs were chosen on the grounds of simplicity of construction both experimentally and in FEM simulations (no particular preference for those designs is implied). The assembly and the specific design of the bridge have shown to have considerable influence on the response of the top plate regarding the mode shapes above 300 Hz. Depending on the geometry of the bridge, its deflections can either be comparable to the maximum deflections of the top plate or can have amplitudes so small that the bridge effectively creates a nodal zone on the plate vibrations. This suggests that the shape, the stiffness, and the mass properties of the bridge may play a role in the sound quality of the instrument.

1. Introduction

The characteristics of the sound generated by a classical guitar depend, in addition to the technique of the player, on the vibratory interaction of the whole instrument to a given string excitation. Among the different parts of a guitar the top plate is the most important in this interaction. The top plate is a few-millimeter-thickness structure that has on the inner face the fan bracing and cross bars, and in the outer face the bridge. The influence of the bridge in the vibrational behaviour of the guitar has been scarcely studied. The few papers that address the role of the bridge in the behaviour of the top plate vibrations contain most of them, only brief commentaries on how the bridge might affect the response of the guitar.

Jovicic [1] measured the responses of four experimental guitar models with structural modifications, and notes that the torque caused by the strings and the presence of the bridge also generate changes in the top plate vibrations, so that the pitch of the instrument depends heavily on the quality and position of the bridge. One indication of this dependency can be obtained from the analysis of energy distribution functions of several pieces of music (and other sounds) played in guitars with different characteristics carried out by Christensen [2], who found that most of the energy comes from regions around 200 Hz and 400 Hz with that from around 400 Hz being greater. In one guitar response interpretation published by Caldersmith [3], he mentioned that the bridge stiffness is often inappropriate and reduces much of the response of the instrument, especially the contribution of the tripolar mode (2, 0), whose nodal lines pass through the wings of the bridge. This mode shape was not present on low quality guitars judged by a group of professional guitarists. Kasha and Kasha [4] report an asymmetrical design (of the fan bracing, the bridge and the hole) of the guitar top plate, arguing that in general all instruments are built asymmetrically (for example, the violin). He points out that the bridge at the endpoint of the strings, is the transmitter of the vibrational energy of the string to the top plate, and so it is advisable to consider the mechanical impedance of the bridge and its frequency dependence. Hill et al. [5], showed how the guitar's input admittance and its sound pressure response at an arbitrary point in its field of radiation, can be characterized and rebuilt using a few acoustic parameters by applying spherical harmonic decomposition. However, this model is not suitable of producing results above 600 Hz. They mentioned that the effective mass of the bridge is significant and that multipolar mode shapes are incompatible with monopolar and bipolar radiation.

We report work done regarding the influence of the bridge on the vibrations of a top plate of a classical guitar. In particular, two geometric versions of the same bridge on a top plate were

* Corresponding author. Tel.: +52 5556228602x1195; fax: +52 5556228606.
E-mail addresses: jesusalejandrott@yahoo.com.mx (J.A. Torres), ricardo.ruiz@ccadet.unam.mx (R.R. Boullosa).

0003-682X/$ - see front matter © 2009 Elsevier Ltd. All rights reserved.
doi:10.1016/j.apacoust.2009.07.002

investigated. The plate vibrations were measured via point mobility (velocity/force) functions. Three cases were studied on the same top plate: the top plate without a bridge, the top plate with a normal bridge attached, and the top plate with the slotted bridge (the cutting was done in situ). These results were compared with those obtained by a damped simulation of the bridge-plate system, for the three configurations, with commercial finite element analysis software. A laser speckle technique was employed, enabling a naked eye visualization that is both simple and easy to implement.

2. Theory

The FEM representation of a continuous structure leads to a matrix system

$$\mathbf{M}\mathbf{x}'' + \mathbf{C}\mathbf{x}' + \mathbf{K}\mathbf{x} = \mathbf{f}(t) \tag{1}$$

where **M**, **C** and **K** are the $n \times n$ matrices containing mass, damping and stiffness terms which are assembled from the individual element matrices. The forcing system is a $n \times 1$ vector $\mathbf{f}(t)$ and the displacements responses are denoted by the $n \times 1$ vector **x**. Modal analysis is carried out when the right side of Eq. (1) is equal to zero, obtaining an undetermined system of equations (one unknown for each degree of freedom and the frequency), which causes the degrees of freedom displacement amplitudes for each mode shape to be expressed in ratios of displacements between them. FEM modal analysis has been widely reported in studies of musical instruments [6–12], and only one work was found with FEM responses functions (admittance) but without experimental validation [11].

If we equate the right side of Eq. (1) with an excitation force defined through its direction, magnitude, location and frequency; the displacements of each degree of freedom are determined by a system with the same number of equations and unknowns, because unlike in modal analysis, the frequency is known. This procedure is called harmonic analysis and Ref. [13] is a guide to how it is carried out by FEM. Moreover, proportional damping ratio from the experimental data was introduced in the calculus obtaining in this way complex Operational Deflection Shapes (ODSs). ODSs depend on the forces or loads applied to a structure and represent the response to a given force at a given point, and unlike mode shapes, they have units (velocity in the present work) and can also be defined for structures that do not resonate [14]. The FEM response functions, and ODSs from the real part, were calculated by harmonic analysis exciting the structure with a swept sinusoidal force with constant amplitude of 1 N. A force was applied at the equivalent point to that used in the experimental setup; the response velocity calculation of the structure was thus comparable to that obtained in the experimental mobility measurements. The model used in FEM calculations did not correspond exactly to the actual boundary conditions of the top plate given by the fixing system structure, which might not have a strictly fixed boundary. The top plate boundary conditions in the simulation were nonetheless specified as zero displacement and rotation for the six degrees of freedom. The other parts of the numerical models have the same length and shape of the experimental top plate; however, the geometric properties of the components can only be reproduced within certain tolerances. Almost all input parameters used in FEM analysis are inexact, at least for two reasons: the pieces cannot be reproduced exactly and because no two pieces of wood are alike, and consequently cannot have the same elastic module. In fact, the scatter of Young's modulus for many materials can often be described as a Gaussian distribution with standard deviation of ±3–5%. The same variation holds true for the loads that are applied to a FEM model [15].

3. Experimental procedures

3.1. The top plate

The measurements were made in an unvarnished top plate, fitted with a Torres traditional fan bracing and under three different conditions: without a bridge, with a bridge attached, and finally with the already attached bridge but cross-cut. The top plate was fixed throughout its contour (except in the area where the fretboard is glued) using a wooden structure shown in Fig. 1 (left), whose walls are considerably more rigid and heavier than those of a guitar. This avoids the coupling of both structures in the frequency range shown in the mobility plots in this work (below 600 Hz). The top fixed plate did not form an air cavity unlike a guitar because of the absence of the back plate. The origin of the coordinate reference system (0, 0) was located at the midpoint of the top plate symmetry line, positive towards the upper bout (X axis) and to the right looking at the bridge (Y axis) as shown in the co-ordinate system in Fig. 1 (center).

From the rectangular wood plate from which the top plate was made, two beams were cut of the remaining material to measure elastic properties of the wood plate: a beam with the length paral-

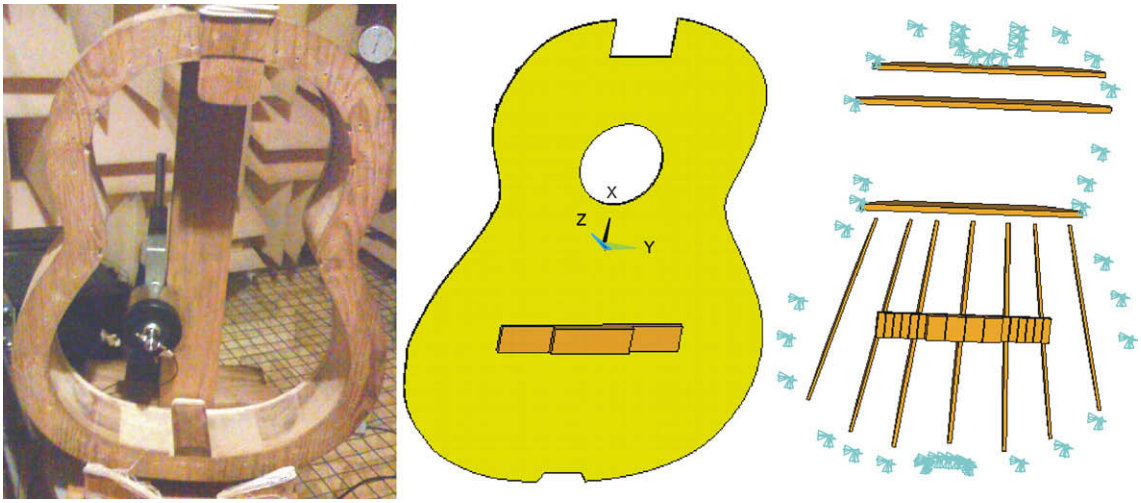

Fig. 1. The guitar top plate. Fixing structure (left), the exciter appears at the back on the bottom left. Top plate geometry and the bridge used in experimental setup and numerical calculations (middle). The top plate was fixed over the fixing structure. The fan bracing and cross-cut bridge appear at the right.

lel to the wood grain (X direction) for the Young's modulus (E) in the longitudinal direction of the plate, and another with a length perpendicular to the grain for E in the transversal direction of the plate (Y direction). The method for determining E in these beams and the fan bracing beams was to find the frequency of the first mode shape freely suspended with longitudinal deflection for each beam, since this frequency depends directly on E, as it is explained in [16]. The values of the shear elastic modulus (G_{XY}) for the plate and the bridge were obtained by finding the frequency of the first mode shape (freely suspended) with torsional deflection for their rectangular plates; a FEM model was used with the corresponding geometry and density. The G modulus of the wood model was changed in the simulation until the frequency matched with the frequency measured for the same torsional mode shape. These procedures are explained in detail in Ref. [17]. In this way, the longitudinal elastic modulus was measured at each piece of wood used, G_{XY} was measured on the plate and bridge woods, and the transversal elastic modulus was measured on the wood for the plate construction. These properties include those considered to be the most important of the wood used in the top plate of the classical guitar [10]. The remaining elastic properties of the wood could not to be obtained. The reason was that the geometry of the wood pieces did not allow the detection of mode shapes proportional to their corresponding elastic properties, as was the case for the transversal dimensions of the fan bracing beams and bridge wood.

3.1.1. The bridge

The bridge was made of a wood that has a density around three times greater than that of the top plate. It also has E_Y 20 times greater than that of the plate. The wood grains in the top plate and the bridge are perpendicular. The same bridge was used in the two cases corresponding to the unmodified and modified bridge. This was done in order to ensure that the same wood and conditions regarding its fixing in the top plate remained the same. To reduce the computing time required, the bridge and its modifications were designed with simplified geometries, shown in Fig. 2 (top). In order to decrease the stiffness of the bridge (longitudinal deflection mainly) each wing of the bridge was modified by doing six spaced cuts; the bridge center was modified with three cuts. These cuts were 1 mm in thickness and left a 2 mm of continuous wood between the line of cuts and the top plate. This modification was chosen only because it is easy to do experimentally and also because it is easier to model in the FEM simulation. The modified bridge is shown in Fig. 2 (bottom). The original bridge had a mass of 34.9 g. The mass loss due to the cross-cuts was of 1.3 g (3.8% mass loss).

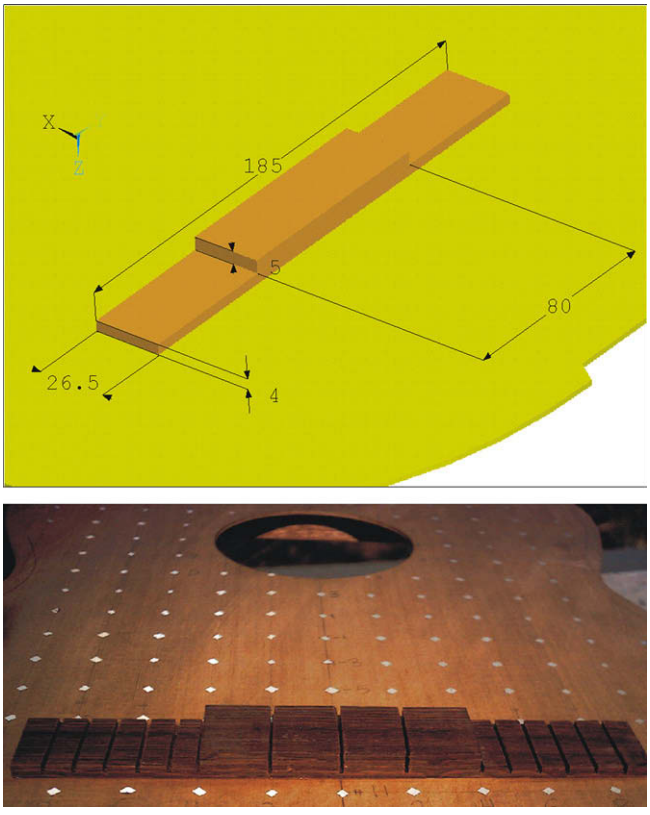

Fig. 2. Bridge geometry configuration. The bridge dimensions (mm) without modifications (top). The bridge with the cross-cut indentations (bottom).

3.2. Excitation and response

Changes in the relative humidity of the air generate variations in the properties of the wood, especially in thin structures such as the top plate [18]. To minimize this effect, the experimental setup was mounted in a chamber where the relative humidity of the air fluctuates less than 1% per day.

The driving point was $(-0.09, -0.06)$ behind the bridge. The excitation signal consisted of white noise with frequency components from 1 Hz to 801 Hz derived from the internal generator output of a two-channel digital signal analyzer (B&K 2034). This signal was sent through a power amplifier (B&K 2706), to an electromagnetic exciter with an impedance head (B&K 8001) attached. The exciter was mounted in a displacement head placed perpendicular to the plane of the top plate with a metallic "stinger". In addition, this configuration allowed the top plate to be excited on the fan bracing face, as shown in Fig. 1 (left) facilitating the visualization techniques of the ODSs in the face with the bridge glued. The mobility was obtained averaging 100 spectra, sending the excitation and the integrated response signals of the impedance head through charge amplifiers (B&K 2615), to the two channels of the analyzer. A set of previous measurements were made to investigate the repeatability of the mobility responses; including the exciter re-location and changes in the response due a force increase. To this end the top plate was mounted, a measurement was made, and then again dismounted. This was repeated three times. The results showed that the changes detected in the resonance frequencies (around ±10 Hz) and amplitudes (around 3 dB) did not change the ODSs geometries or the general mobility appearance.

3.3. Laser vibrometer measurements

A laser vibrometer (B&K 2815) was used to measure the normal velocity in 273 points of a 2×2 cm grid, using small pieces (2×2 mm) of reflective tape glued at each point of the grid except in the bridge position. A partial view of this mesh can be seen in Fig. 2 (bottom). The co-ordinates of the 273 points were sorted in a spatial matrix to view the vibration of the top plate from their velocities corresponding to a specific frequency, similar to the configuration used by Le Pichon et al. [19]. The velocity measurements of the whole surface were performed in about 2 h.

3.4. Naked eye visualization

A technique considerably easier to implement using naked eye visualization to identify the ODSs was applied [20]. Basically a vibrating area is illuminated by a beam of laser light, made divergent in order to cover the whole surface; in our case with a ball lens of 3 mm of diameter and 2.2 mm of focal length. A tilt of the surface due to a gradient in the normal component of dis-

placement, caused by the normal vibration of the surface will cause a movement of a bright area (in the interference pattern). During a complete cycle of the vibration it will move the bright area laterally through a distance approximately equal to its width (for a differential displacement equal to $\lambda/2$ of the laser light). The threshold vibration level at which the streaks appear is that amplitude for which the peak difference in displacement for points on the surface separated by the diameter of the spot area is just $\lambda/2$. For distances greater than $\lambda/2$ and for frequencies to high to be resolved by the human eye, the pattern areas corresponding to the tilting surface areas will be streaked in a direction parallel to the gradient of the displacement [21]. It was corroborated in this work that it is a difficult task [22] to photograph the laser-streak patterns, because the laser reflection from the wood is not enough to capture the phenomenon. The spots from the reflective dots of the grid mentioned in Section 3.3, aids the photographing process of the laser-streak pattern. The camera must to be as close as possible to the laser in order to capture the reflection from the tape (Fig. 3, left), because the reflection is in the same direction as the incident light. Each dot generates a laser-streak pattern, and it can be made more pronounced in order to be photographed by defocusing the observed grid. The circles appearing correspond to the non-focused photographs of the reflective dots of the grid in Fig. 3 (right). The method of using the reflections of the grid dots has shown to be a significant improvement over the standard technique in photographing the speckle-streak phenomenon.

In antinodal zones, the lines of the streak pattern present a sudden change of direction. To illustrate this, Fig. 4 shows a set of normal vectors to the surface of the lower mode shape of a top plate (left). If the top plate is viewed along the Z axis towards the XY plane (center), one sees a pattern similar in detail to the photograph from the non-focused reflections of the tape (right).

4. Results

4.1. Experimental and numerical mobility

Fig. 5 shows the experimental (solid line) and the damped simulated (dashed line) mobility in decibels referenced to 1 (m/s)/N, of the top plate without bridge. Four resonance peaks can be clearly discerned. A proportional damping ratio of 0.02 was measured from the two experimental resonance peaks and this value was applied to their FEM calculus. The third experimental resonance peak diminishes its damping ratio to 0.01, thus this value was used in its corresponding FEM calculus. Moreover, this FEM simulation with 0.01 damping ratio gave a better resemblance to the experimental mobility at the anti-resonance between the first two resonances. In the FEM simulation of the fourth experimental resonance peak, a value of 0.02 damping ratio was used instead of the measured value of 0.01. This damping increase in the FEM calculus was made to compensate a lower experimental peak amplitude, attributed to the influence of the exciter's mass and stiffness in the corresponding ODS because the exciter position was in an antinodal point. The FEM calculus generated thus a fourth resonance peak with amplitude close to the experimental data, but the price to pay was a wider peak. By adjusting the unmeasured elastic properties of the wood in the FEM calculus the simulated response was made to be similar to the experimental curve as shown in the figure.

4.2. Operational deflection shapes visualization

Fig. 6 shows the ODSs corresponding to the second and third resonance peaks of the mobilities of Fig. 5 (the first resonance was shown in Fig. 4). The images from the FEM calculus (bottom) are shown with level curves and polarities of the relative displacements in the top plate. The vectors plotted were obtained by calcu-

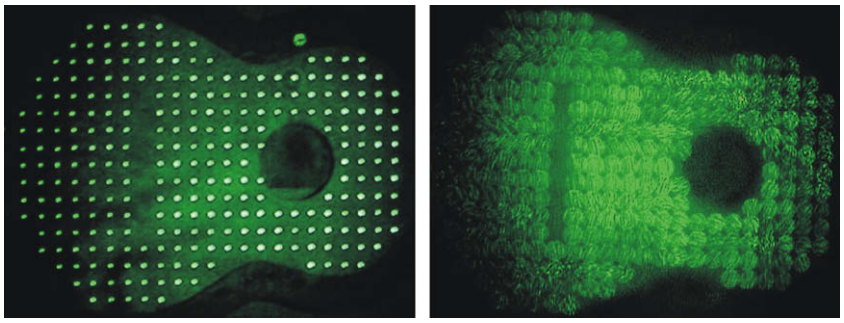

Fig. 3. Defocusing the grid pattern. The grid (left) is defocused in order to capture the laser-streak pattern (right).

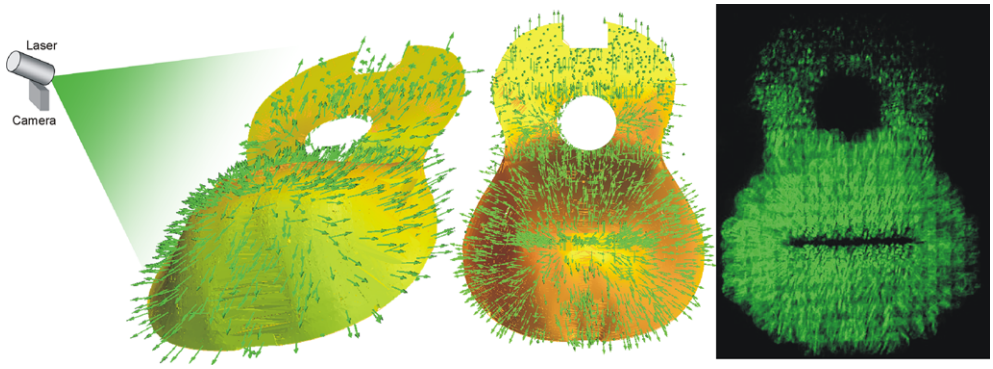

Fig. 4. Laser-streak pattern. The non-focused reflections of the tape generate a laser-streak pattern (right) that corresponds to the projection in the XY plane (center) of the normal vectors to the deformed surface (left).

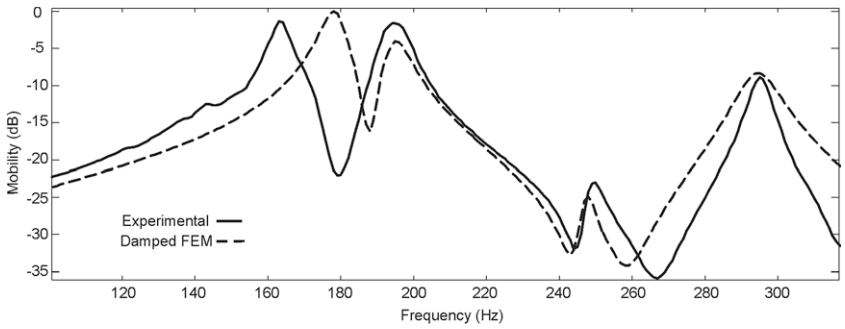

Fig. 5. Experimental and numerical mobility. Typical mobility curve of the top plate without bridge, obtained experimentally (solid line) and from FEM data (dashed line).

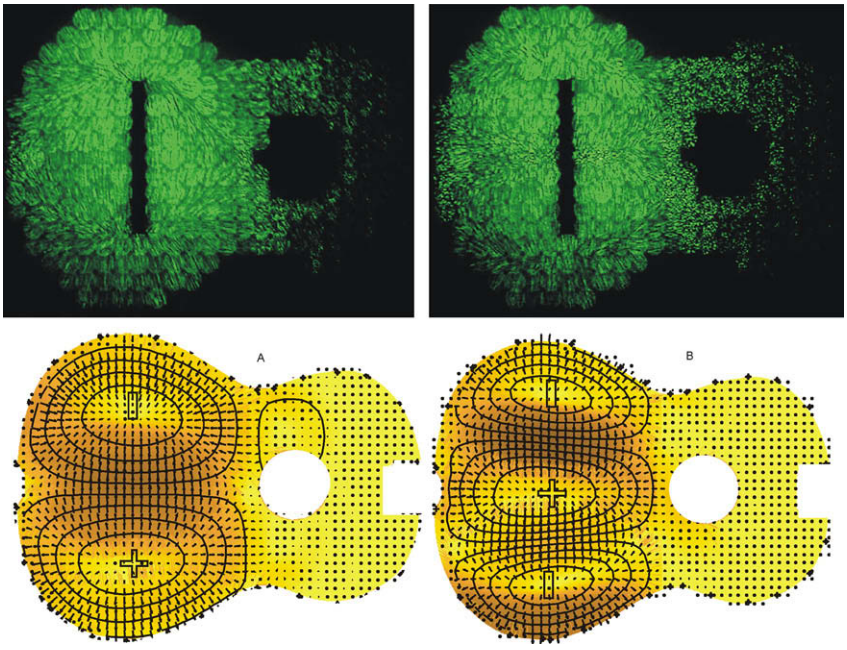

Fig. 6. Second and third resonance. Photographs corresponding to the second and third resonance peaks of the top plate without bridge displayed by naked eye identification technique (top), and the gradient of the out-of-plane displacement from FEM data (bottom).

lating the gradient of the simulated surface deflection. Moreover, shaded top plates are included for each case in order to facility the interpretation of the corresponding photographs (top).

Fig. 7 shows the normal velocity to the surface of the ODS corresponding to the fourth resonance peak, forced by 0.035 N (at 293 Hz) obtained experimentally with a vibrometer (right), and the FEM mesh (left). To verify the consistency between both procedures, the modal assurance criterion (MAC) was calculated. The MAC value is between 0 and 1 regardless of the scale of the values to compare. A MAC value of 1 means that a modal vector is a multiple of the other [23]. The MAC value for the ODSs shown in Fig. 7 was 0.82, and the magnitudes of velocities in both cases were similar, subjected to the same level of excitation, as can be seen in their colorbars (m/s).

5. Discussion

Fig. 8 shows the measured point mobility at the top plate with bridge (solid line) and with the cross-cut bridge (dashed line). Despite the fact that the general geometry of the ODSs on the top plate with bridge and the cross-cut bridge was almost the same, the assembly and modification of the bridge caused considerable changes in the response of the top plate. The most notable change was a frequency decrease of the third lower resonance peak (at 66 Hz), and the presence of an ODS with five anti-nodal zones (here referred to as poles) in the response with the cross-cut bridge in the frequency range shown.

The numerical model was useful in comparing specific changes in the properties of the structure due to changes in the bridge geometry, the others conditions remaining unchanged; or by changing a physical property and keeping the same geometry. A simulated top plate mobility response was calculated using a mass 3.8% lower than the real mass by removing the mass loss due to the cross-cutting of the bridge as was mentioned in Section 3.1.1. This mass change was made through a density decrease, not by a geometry modification. Another mobility response was calculated adding the mass removed due the cuts, via a density increase in the cross-cut bridge. Four mobilities were thus obtained: one for each bridge design (normal and cross-cut bridge) weighting 34.9 g, and two more of both weighting 33.6 g. It was clear that the variations in the response of the top plate due to the two bridge models, were more pronounced due to the change brought about by the cross-cuts than by the mass decrease.

Another FEM application was the calculation of ODSs. These data helped to obtain geometric models of the deflections of all parts of the structure, including the cut an uncut bridge. In the

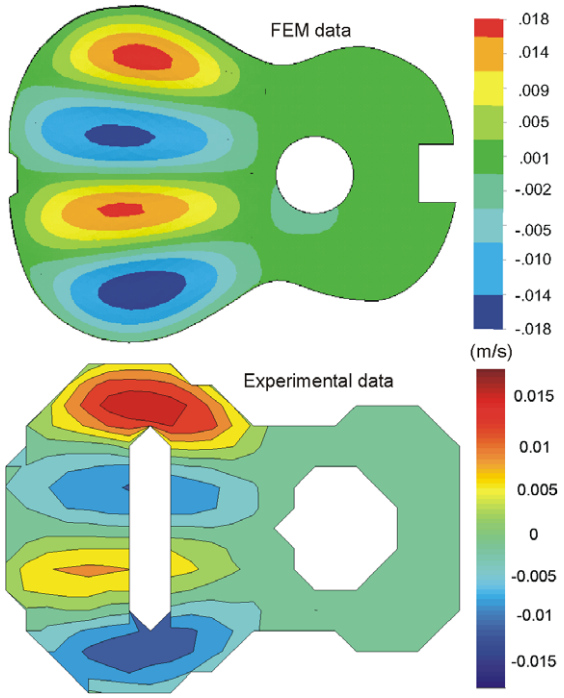

Fig. 7. Operational deflection shape. Comparison of simulated (top), and experimental (bottom), ODS of the top plate velocity without bridge in its fourth resonance peak excited with 0.035 N (MAC = 0.82).

two lowest ODSs in resonance condition, both bridge designs remain almost rigid. The ODS of the top plate corresponding to the first resonance appears flattened in the central region (Fig. 9A). In the second resonance peak the bridge moves as a "balance beam" on the axis of the dipole. Its maximum displacements points are further between them and are closer to the ends of the bridge (Fig. 9B) than for the case of the dipole without bridge (Fig. 6B). For the case of the cut bridge, the frequency and amplitude of the second resonance peak increase. At higher frequencies, the response starts to be more affected because by the bridge either because it is deformed or because it imposes a nodal zone in the ODS.

Both bridge designs are deformed in the ODS corresponding to the third resonance peak; this shape corresponds to the tripole mode shape. But its frequency gets lower (decoupling with the next peak) and its amplitude increases in the case of the cut bridge, probably because of the loss of stiffness and damping. The corresponding ODS of the top plate without bridge presents almost the same maximum velocities in the three poles. The normal bridge presence causes a widening of the middle pole; its maximum velocity is one third of the maximum velocities of the outer poles (Fig. 9C). The cuts in the bridge generate a less pronounced widening effect on the middle pole; the ratio between the maximum velocity from the middle pole and the maximum velocities of the outer poles now increases to one half. Variations in the third resonance peak have particular interest, because its notorious contribution to the guitar sound radiation has already been reported [24,25].

The deflection in both bridges for the fourth resonance peak ODS (Fig. 9D) is less pronounced than the previous peak (Fig. 9C) due to a similar effect of the second resonance (Fig. 9B), but the cuts led to a slight decrease in the frequency of the resonance peak and a corresponding increase in its amplitude (about 3 dB) which can be attributed to stiffness and mass loss caused by the bridge cuts. Comparing Fig. 9D with Fig. 7, one observes that the bridge diminishes the response of the middle poles with respect to that from the outer poles: the maximum velocity was not reached like in the top plate without bridge, where the maximum velocities in the four poles were almost the same. The cuts in the bridge do not considerably modify this ODS, except for the shape of the middle poles that were somewhat smoother than those observed with the normal bridge.

In the ODS corresponding to the fifth resonance peak, the bridge deflection is so pronounced by the bridge modification (Fig. 9E), that the resonance peak becomes clearly distinguishable in the frequency range of the mobility response, in contrast to the case of the uncut bridge. After this resonance, in the next ODS calculated with the FEM model (Fig. 9F), the bridge has a moderate torsional deflection and a nodal line is crossing it. The excitation in the position behind the bridge did not allow a clearly detection of this six-pole ODS in the experimental measurements.

In order to have some sense of the possible effects that this might bring to the sound of the guitar a simple test was made. A recording of three arpeggios of an *E* chord (in a guitar from one of the authors) was made with two microphones at around 30 cm from the sound hole. Then the bridge was slotted with five cuts, and another recording was made. Some changes that might have occurred were barely audible to the authors and cannot be attributed directly to the change in the bridge; they might have been a consequence of the way the strings were excited (by hand). These opinions were corroborated submitting the audio file to 20 persons with the task of hearing them and look for a change in the sound; no clear consensus was reached. It seems that the reduction in stiffness of the bridge does not reduce the strength of the top plate supporting the tension of the strings. This is supported by the fact that some guitars have been constructed with slotted bridges [4,26].

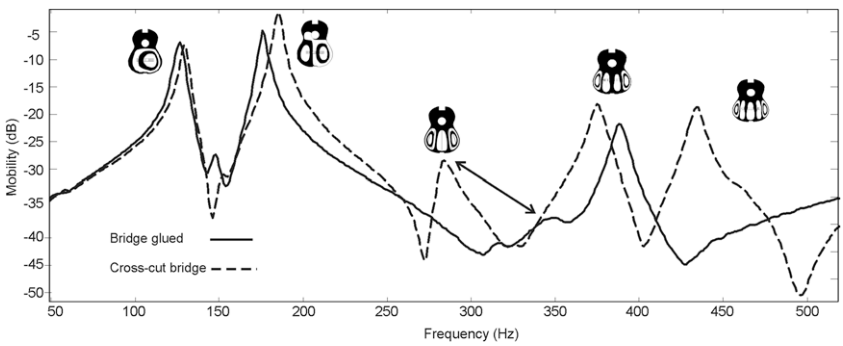

Fig. 8. Changes in the mobility due to the modified bridge. Experimental mobility and resonance peaks ODSs of the top plate with bridge (solid line) and with cross-cut bridge (dashed line).

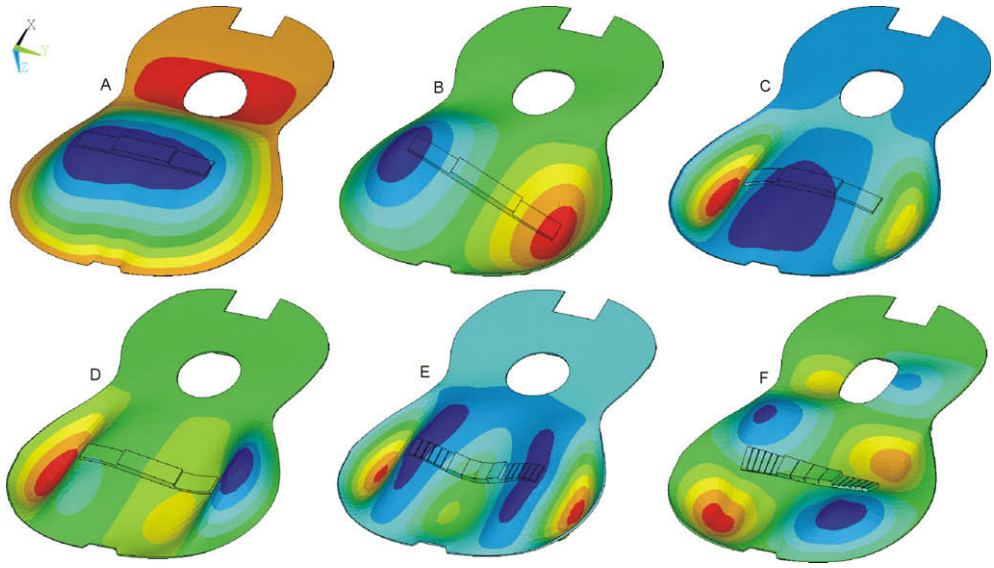

Fig. 9. General behaviour of the bridge in six resonances of the top plate. The lowest ODS shown in resonance condition is denoted with an A, and the higher with an F.

6. Conclusions

The influence of two bridge configurations in the top plate response of a classical guitar was analyzed, the primary goal of this work. The presence of the bridge in the top plate changed significantly the structural response of the plate-bridge system. In turn, changes in the stiffness and mass of the bridge helped to identify those operational deflection shapes that are more sensitive to these changes. These results show that a simple change in the structural configuration, here realized by the simple expedient of cross-cutting the bridge has noticeable effects in the vibration patterns. It was shown in particular that the tripole mode is greatly enhanced in displacement amplitude, and is accompanied by a lowering of its frequency of vibration. How this affects the overall radiation or the quality of the tone of the guitar remains to be seen, a clear audible change was not discerned in a simple test. Two non-standard techniques were applied to visualize some operational deflection shapes of the top plate: speckle naked eye visualization, and damped FEM harmonic analysis. The FEM velocity mesh had an 82% of agreement with the experimental data obtained with a laser vibrometer as measured by the modal assurance criterion, for a given frequency. The laser-streak patterns viewed with the naked eye technique was enhanced and was successfully photographed. A problem that has been a drawback of this non-standard technique. The photographs were compared with the calculated gradient of the deformed surface of the top plate and showed good agreement. This technique is easy to implement and offers an inexpensive dynamic testing method.

References

[1] Jovicic JO. Le role des barres de raidissement sur la table de resonance de la guitare: II. Leur effet sur les nodales de la table (etude holographique). Acustica 1977;38:15–6.
[2] Christensen O. The response of played guitars at middle frequencies. Acustica 1983;53:107–26.
[3] Caldersmith G. The guitar frequency response. J Guitar Acoust 1982;6:1–9.
[4] Kasha M, Kasha N. Applied mechanics and the modern string instrument–classical guitar. J Guitar Acoust 1982;6:105–21.
[5] Hill TJW, Richardson BE, Richardson SJ. Acoustical parameters for the characterization of the classical guitar. Acta Acust Acust 2004;90:335–48.
[6] Marshall K. Modal analysis of a violin. J Acoust Soc Am 1985;77(2):695–709.
[7] French M, Lewis K. Modal analysis of an acoustic guitar. In: Proc. int. modal an., Nashville; 1995.
[8] Richardson BE, Walker GP. Predictions of the sound pressure response of the guitar. Proc Int OA 1987;9(3):43–6.
[9] Bissinger G. Some mechanical and acoustical consequences of the violin soundpost. J Acoust Soc Am 1995;97(5):3154–64.
[10] Ezcurra A. Influence of the material constants on the low frequency modes of a free guitar plate. J Sound Vib 1996;194(4):311–22.
[11] Elejabarrieta MJ, Ezcurra A, Santamaría C. Vibrational behaviour of the guitar soundboard analysed by the finite element method. Acta Acust Acust 2001;87:24–8.
[12] Okuda A, Ono T. Bracing effect in a guitar top board by vibration experiment and modal analysis. Acoust Sci Technol 2008;29(1):103–5.
[13] Torres D. Simulación de la Microscopía de Fuerza Modulada por el Método del Elemento Finito. Master Thesis, CINVESTAV; 2005.
[14] Richardson MH. Is it a mode shape, or an operating deflection shape? Sound Vib 1997:1–11.
[15] Probabilistic design techniques. In: ANSYS release 8.0 Documentation; 2004.
[16] Caldersmith G. Vibration theory and wood properties. J Catgut Acoust Soc 1984;42:4–11.
[17] Torres JA. Modos de vibración simulados por computadora y experimentales de una tapa de guitarra en sus etapas de construcción. Master Thesis, CCADET UNAM; 2006.
[18] Panshin AJ, de Zeeuw C. Textbook of wood technology. Part 1. Formation, anatomy, and properties of wood. New York: McGraw-Hill; 1980.
[19] Le Pichon A, Berge S, Chaigne A. Comparison between experimental and predicted radiation of a guitar. Acta Acust Acust 1998;84:3–17.
[20] Torres JA, Boullosa RR. Identificación A Simple Vista De Patrones De Vibracion De Una Tapa De Guitarra. In: Congr Acust, 2008, Coimbra, Portugal. <http://www.sea-acustica.es/Coimbra08/id031.pdf>.
[21] Massey GA. Study of vibration measurement by laser methods. NASA Rept No. NASA-CR-75643; 1965. p. 32–9.
[22] Fernelius N, Tome C. Vibration analysis studies using changes of laser speckle. J Opt Soc Am 1971;61(5):566–73.
[23] Friswell MI, Mottershead JE. Finite element model updating in structural dynamics. 1st ed. Netherlands: Kluwer Academic Publishers; 1995.
[24] Caldersmith G. Radiation from lower guitar modes (musical acoustics). Am Luth 1985;2:20–4.
[25] Lai JCS, Burgess MA. Radiation efficiency of acoustic guitars. J Acoust Soc Am 1990;88:563–9.
[26] Eban G. The relation of musical acoustics research to guitar design and building. In: Int. Symp. mus. acoust.; 1998. Washington, USA.